X. BİLSEL ULUSLARARASI DÜNYA BİLİM ve ARAŞTIRMA KONGRESİ

09-10 Mayıs 2026

KONGRE KİTABI

BİLSEL YAYINCILIK

İSTANBUL

https://bilselkongreleri.com

10. BİLSEL INTERNATIONAL WORLD SCIENCE AND RESEARCH CONGRESS BOOK

May 09-10, 2026
İSTANBUL/TÜRKİYE

EDITOR
Assoc. Prof. Dr. İlyas ERPAY

ISBN: '978-625-8531-30-5'

https://bilselkongreleri.com/

25 MAY, 2026

PARAMETRİC ASSESSMENT OF A SOLAR-DRİVEN COMBİNED COOLİNG, HEATİNG, AND POWER (CCHP) PLANT İN LİBYA

Abdulhakim ALDIGHEES[1], Emrah DENİZ[2], Abdulrazzak AKROOT[3]

[1] Master's Student, Department of Mechanical Engineering, Faculty of Engineering and Natural Sciences, Karabük University, 78050 Karabük, Turkey. ORCID iD: https://orcid.org/0009-0002-8688-2683

[2] Department of Mechanical Engineering, Faculty of Engineering and Natural Sciences, Karabük University, 78050 Karabük, Turkey. ORCID iD: https://orcid.org/0000-0003-0182-2631

[3] Department of Mechanical Engineering, Faculty of Engineering and Natural Sciences, Karabük University, 78050 Karabük, Turkey. ORCID iD: https://orcid.org/0000-0002-1561-7260

Corresponding author: abdulrazzakakroot@karabuk.edu.tr

Abstract

This study presents a parametric assessment of a solar-driven combined cooling, heating, and power (CCHP) plant designed for power, cooling, and heating production under the climatic conditions of Tripoli, Libya. The proposed configuration integrates a solar-assisted regenerative Brayton cycle as the topping cycle, a regenerative organic Rankine cycle (ORC) for additional power generation, a single-effect LiBr–H_2O absorption refrigeration system for cooling production, and a heat recovery unit for useful hot-water generation. The system is evaluated from energy, exergy, exergoeconomic, and environmental perspectives to determine its thermodynamic performance, cost effectiveness, and potential contribution to sustainable energy production. The base-case results show that the Brayton cycle produces 5023 kW, while the ORC contributes 1291 kW, resulting in a net power output of 6314 kW. The system also provides 2892 kW of cooling and 613.2 kW of heating, with an overall energy utilization factor of 67.3% and an overall exergy efficiency of 45.31%. The absorption refrigeration subsystem achieves a coefficient of performance of 0.807. The economic results indicate a total product cost of 23.44 \$/MWh and a net electricity cost of 23.85 \$/MWh, while the normalized CO_2 emission is 1.42 kg CO_2/MWh. Parametric results reveal that increasing the Brayton pressure ratio improves net power output and exergy efficiency but reduces heating capacity and increases specific CO_2 emissions. Increasing the ORC turbine inlet temperature slightly enhances power output, efficiencies, and economic and environmental performance. Overall, the proposed solar-driven CCHP plant demonstrates promising potential for sustainable multigeneration applications in Libya and similar solar-rich regions with high cooling demand.

Key Words: Solar energy; CCHP plant; Parametric assessment; Organic Rankine cycle; Libya.

Özet

Bu çalışma, Libya'nın Trablus kentinin iklim koşulları altında güç, soğutma ve ısıtma üretimi için tasarlanan güneş enerjili birleşik soğutma, ısıtma ve güç üretim (CCHP) santralinin parametrik değerlendirmesini sunmaktadır. Önerilen sistem; üst çevrim olarak güneş destekli rejeneratif Brayton çevrimini, ilave güç üretimi için rejeneratif Organik Rankine Çevrimi'ni (ORC), soğutma üretimi için tek etkili LiBr–H_2O absorpsiyonlu soğutma sistemini ve faydalı sıcak su üretimi için bir ısı geri kazanım ünitesini entegre etmektedir. Sistem; enerji, ekserji, eksergoekonomik ve çevresel açılardan değerlendirilerek termodinamik performansı, maliyet etkinliği ve sürdürülebilir enerji üretimine katkı potansiyeli belirlenmiştir. Temel durum sonuçları, Brayton çevriminin 5023 kW güç ürettiğini, ORC'nin ise 1291 kW ilave güç sağladığını ve böylece toplam net güç çıktısının 6314 kW'a ulaştığını göstermektedir. Sistem ayrıca 2892 kW soğutma ve 613,2 kW ısıtma sağlamaktadır. Genel enerji kullanım faktörü %67,3, genel ekserji verimi ise %45,31 olarak elde edilmiştir. Absorpsiyonlu soğutma sisteminin performans katsayısı 0,807 olarak bulunmuştur. Ekonomik sonuçlar, toplam ürün maliyetinin 23,44 $/MWh ve net elektrik üretim maliyetinin 23,85 $/MWh olduğunu, normalize CO_2 emisyonunun ise 1,42 kg CO_2/MWh olduğunu göstermektedir. Parametrik sonuçlar, Brayton basınç oranındaki artışın net güç çıktısını ve ekserji verimini artırdığını, ancak ısıtma kapasitesini azalttığını ve özgül CO_2 emisyonlarını yükselttiğini ortaya koymaktadır. ORC türbin giriş sıcaklığının artırılması ise güç çıktısını, verimleri ve ekonomik-çevresel performansı sınırlı düzeyde iyileştirmektedir. Genel olarak, önerilen güneş enerjili CCHP santrali, Libya ve yüksek soğutma talebine sahip benzer güneş potansiyeli yüksek bölgeler için sürdürülebilir çoklu üretim uygulamaları açısından umut verici bir potansiyel göstermektedir.

Anahtar Kelimeler: Güneş enerjisi; CCHP santrali; Parametrik değerlendirme; Organik Rankine çevrimi; Libya.

1. INTRODUCTION

The increasing demand for electricity, cooling, and heating has encouraged the development of integrated energy systems that can produce multiple useful outputs from a single energy source. Combined cooling, heating, and power (CCHP) systems are considered promising solutions because they improve overall energy utilization by recovering and reusing waste heat that would otherwise be rejected to the environment (Cho et al., 2014; Shi et al., 2017; Wu & Wang, 2006). Compared with conventional separate production systems, CCHP plants can achieve higher efficiency, lower fuel consumption, and reduced environmental impact (Liu et al., 2014).

Solar energy is one of the most attractive renewable energy sources for driving CCHP systems, especially in regions with high solar radiation (Wang et al., 2020; Zhang et al., 2017). Libya has strong solar potential due to its geographical location and long sunshine duration, making solar-driven multigeneration systems a suitable option for sustainable energy development (Eshtaiwi et al., 2022; Khalil et al., 2017). In particular, Tripoli has favorable climatic conditions that can support the application of solar-assisted power and cooling technologies, especially because cooling demand is high in hot regions (Gnedi & Robaa, 2024; Tawil et al., 2018).

Several previous studies have investigated solar-driven CCHP and trigeneration systems using different thermodynamic configurations. (Wang et al., 2009) proposed one of the early solar-driven CCHP systems by combining a Rankine cycle with an ejector refrigeration cycle to produce power, cooling, and heating simultaneously. (Pokson & Chaiyat, 2022)examined the thermal performance of a CCHP system that recovers energy from infectious medical waste to produce cooling, heating, and power. (Zhang et al., 2017) analyzed a solar-assisted CCHP system and evaluates its potential to improve energy efficiency by integrating solar energy into CCHP operation. (Akroot et al., 2026) analyzed a solar-assisted combined cooling, heating, and power system designed for smart-city applications in Doha, Qatar. It highlighted the suitability of solar-driven CCHP systems for regions with high solar radiation and strong cooling demand. (Shi et al., 2017) focused on the modeling, optimization, and operational strategies of CCHP systems to improve their overall energy, economic, and environmental performance. (Akroot & Refaei, 2025) presented a thermodynamic and exergoeconomic assessment of a solar-assisted combined cooling, heating, and power system in Antalya, Turkey. It focuses on evaluating how integrating solar energy can improve system efficiency, reduce energy losses, and enhance the economic performance of CCHP operation in a region with strong solar potential. (L. Zhao et al., 2018) compared sequential and parallel configurations of solar-driven ORC-based CCHP systems, highlighting the importance of system arrangement in improving overall performance. (Zarei et al., 2021) conducted energy, exergy, and economic analyses of a multi-source solar-driven CCHP system, confirming the value of integrated renewable configurations for efficient multigeneration. (García-Domínguez et al., 2023) analyzed a solar-driven ORC–absorption CCHP system using a detailed exergy approach, while (Jiménez-García et al., 2024) studied a solar-driven ORC–absorption cooling system for simultaneous power and cooling production. (X. Zhao et al., 2024) optimized a solar-powered ORC–VCR–CCHP system using a ternary refrigerant selection model. (Aieneh et al., 2024) also investigated a solar-powered CCHP plant integrated with water electrolysis using energy, exergy, and exergoeconomic assessments. In addition, recent studies have continued to examine solar-assisted CCHP systems with ORC, absorption refrigeration, and hybrid renewable inputs, showing that such systems can reduce fossil-fuel dependence and improve energy sustainability in regions with high solar potential. These studies provide a strong foundation for the present work, which focuses on the parametric assessment of a solar-driven Brayton–ORC–absorption CCHP system under the climatic conditions of Tripoli, Libya.

In this study, a solar-driven CCHP system is proposed and analyzed for power, cooling, and heating production under the climatic conditions of Tripoli, Libya. The proposed configuration consists of a solar-assisted regenerative Brayton cycle as the topping power cycle, a regenerative organic Rankine cycle (ORC) for additional electricity generation, a single-effect LiBr–H_2O absorption refrigeration system for cooling production, and a heat recovery unit for useful heating. This integrated arrangement allows solar thermal energy to be used in a cascade manner, beginning with power generation and continuing with cooling and heating production.

2. SYSTEM DESCRIPTION

Figure 1 illustrates the schematic layout of the proposed solar-driven combined cooling, heating, and power (CCHP) system designed for operation under the climatic conditions of Tripoli, Libya. The system integrates a solar-assisted regenerative Brayton cycle as the topping power cycle, a regenerative organic Rankine cycle (ORC) for additional electricity generation, a single-effect LiBr–H_2O absorption refrigeration cycle for cooling production, and a heat recovery unit for useful hot-water generation. Solar energy collected by the heliostat field is converted into high-temperature thermal energy in the solar receiver and supplied to the Brayton cycle. The remaining thermal energy from the Brayton exhaust is then sequentially recovered to drive the ORC, the absorption cooling subsystem, and the heating unit. This cascade arrangement enables the effective utilization of solar-derived heat for simultaneous power, cooling, and heating production, thereby improving the overall energy utilization of the proposed CCHP plant.

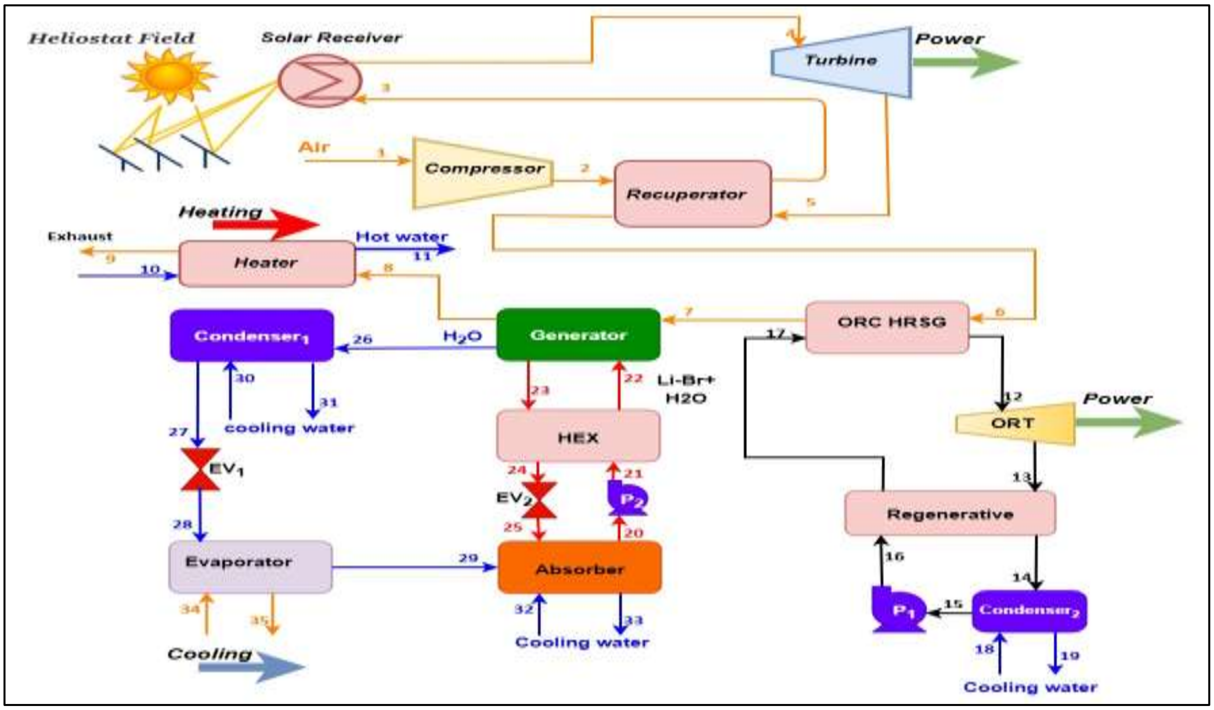

Figure 1: Schematic diagram of the proposed solar-driven combining cooling, heating, and power (CCHP) system.

The thermodynamic model of the proposed solar-driven combined cooling, heating, and power (CCHP) system was developed based on the following assumptions (Alfaris et al., 2025; Kareem et al., 2023; P.P. da Silva et al., 2025; X. Zhao et al., 2024):

- All thermodynamic properties and mass flow rates are assumed constant with time.
- Changes in kinetic and potential energies are neglected for all components because they are very small compared with thermal and mechanical energy changes.

- The compressor, gas turbine, ORC turbine, and pumps are modeled using constant isentropic efficiencies.
- The organic working fluid in the ORC is assumed to leave the condenser as a saturated liquid.
- Pressure drops in pipes, heat exchangers, and other connecting components are neglected unless otherwise specified.
- The LiBr–H_2O absorption cycle operates at steady thermodynamic equilibrium, and the refrigerant is pure water while lithium bromide acts as the absorbent.
- The refrigerant leaving condenser is assumed to be a saturated liquid, whereas the refrigerant leaving the evaporator is assumed to be a saturated vapor.
- The expansion valves, EV_1 and EV_2, are assumed to operate under isenthalpic throttling conditions.

The solar radiation input is represented by the selected direct normal irradiance value for Tripoli, Libya, and the heliostat field is assumed to supply thermal energy continuously under the defined design conditions.

Table 1 summarizes the main input parameters and operating conditions adopted for the simulation and performance assessment of the proposed solar-driven combined cooling, heating, and power (CCHP) system. These parameters define the baseline design of the integrated plant, including the operating conditions of the Brayton cycle, the specifications of the heliostat field, and the key temperature and concentration settings of the LiBr–H_2O absorption cooling subsystem. The listed values provide the foundation for the thermodynamic, exergetic, exergoeconomic, and environmental analyses and are used to evaluate the system performance under the selected design conditions for Tripoli, Libya.

Table 1. Input values utilized for the design of the solar-driven CCHP system

Component	Parameter	Value
Brayton cycle	Pressure ratio	10
	Compressor's inlet temperature	28℃
	Compressor's inlet pressure	1 bar
	Compressor's isentropic efficiency	82%
	Air flow rate	26 kg/s
	Turbine's isentropic efficiency	87%
Heliostats field	Area	27000 m2
	Location	Tripoli- Libya
	Latitude	32.8874° N
	Longitude	13.1873° E
	DNI	750 W/m2
LiBr–H_2O absorption cooling cycle	Condenser temperature (T18)	38 ℃
	Generator temperature (T14)	85 ℃
	Absorber temperature (T11)	36 ℃
	SHEX effectiveness	55 (%)
	Evaporator temperature (T19)	6 ℃
	LiBr Solution strength (%)	53 (%)

The numerical simulation of the proposed solar-driven CCHP system was carried out using Engineering Equation Solver (EES). The software was employed to solve the governing thermodynamic equations, calculate the thermophysical properties of the working fluids, and evaluate the energy, exergy, exergoeconomic, and environmental performance indicators. By using the input parameters listed in Table 1, EES enabled a consistent simulation of the integrated Brayton, ORC, absorption cooling, and heating subsystems under the selected design conditions.

The thermodynamic equations were used to evaluate the energy and exergy performance of the proposed solar-driven CCHP system under the selected operating conditions. These equations form the basis for calculating power output, cooling capacity, heating load, efficiency indicators, and exergy destruction.

The power output of the Brayton cycle is calculated from the difference between the gas turbine work and the compressor work.

$$\dot{W}_{BC} = \dot{W}_{GT} - \dot{W}_{AC} \quad (1)$$

The power generated by the organic Rankine cycle is determined based on the net work produced by the ORC turbine after accounting for the pump power consumption.

$$\dot{W}_{ORC} = \dot{W}_{ORT} - \dot{W}_{P1} - \dot{W}_{P2} \quad (2)$$

The total net power output of the proposed CCHP system is obtained by combining the useful power produced by the Brayton cycle and the ORC subsystem.

$$\dot{W}_{net} = \dot{W}_{GT} - \dot{W}_{AC} + \dot{W}_{ORT} - \dot{W}_{P1} - \dot{W}_{P2} \quad (3)$$

The cooling capacity of the absorption refrigeration subsystem is evaluated from the heat absorbed in the evaporator (Akroot, 2025).

$$\dot{Q}_{Cooling} = \dot{Q}_{Evap} \quad (4)$$

The useful heating capacity is calculated based on the recovered thermal energy supplied to the heating unit.

$$\dot{Q}_{Heating} = \dot{Q}_{Heater} \quad (5)$$

The overall energy utilization factor is used to assess the fraction of the input solar energy converted into useful power, cooling, and heating products.

$$EUF = \frac{\left(\dot{W}_{net} + \dot{Q}_{Cooling} + \dot{Q}_{Heating}\right)}{\dot{Q}_{Solar}} \quad (6)$$

The electrical energy utilization factor represents the share of the input energy that is converted into net electrical power (Talal & Akroot, 2023).

$$EUF_{ele} = \frac{\dot{W}_{net}}{\dot{Q}_{Solar}} \quad (7)$$

The exergy associated with the heating product is calculated to determine the useful work potential of the recovered thermal energy.

$$\dot{E}_{Heating} = \dot{Q}_{Heating}\left(1 - \frac{T_o}{T_h}\right) \quad (8)$$

The exergy of the cooling product is evaluated to quantify the useful effect produced by the absorption refrigeration cycle.

$$\dot{E}_{Heating} = \dot{Q}_{Cooling}\left(\frac{T_o}{T_h} - 1\right) \quad (9)$$

The overall exergy efficiency is used to measure how effectively the input exergy is converted into useful power, cooling, and heating outputs .

$$\eta_{ex} = \frac{\left(\dot{W}_{net} + \dot{E}_{Cooling} + \dot{E}_{Heating}\right)}{\dot{E}_{solar}} \quad (10)$$

The electrical exergy efficiency indicates the effectiveness of the system in converting the supplied exergy into net electrical power.

$$\eta_{ex,ele} = \frac{\dot{W}_{net}}{\dot{E}_{solar}} \quad (11)$$

The total exergy destruction is calculated to identify the overall irreversibilities occurring within the integrated CCHP system (Deniz & Çınar, 2016; Talal & Akroot, 2024).

$$\dot{E}_{d,total} = \sum \dot{E}_{D,k} \quad (12)$$

The unit exergy cost of the total product is determined to evaluate the exergoeconomic performance of all useful outputs produced by the system.

$$c_{Prod} = \frac{\dot{C}_{Prod}}{\dot{E}_{Prod}} \quad (13)$$

The unit exergy cost of electricity is calculated to estimate the cost associated with the net electrical power generated by the system.

$$\dot{E}_{Prod} = \dot{W}_{net} + \dot{E}_{Cooling} + \dot{E}_{Heating} \quad (14)$$

The unit cost of electricity is determined as the ratio of the total product cost rate to the net electrical power generated by the proposed CCHP system.

$$c_{ele} = \frac{\dot{C}_{Prod}}{\dot{W}_{net}} \quad (15)$$

The normalized CO_2 emission is calculated by dividing the CO_2 emission rate by the net power output of the system (Alfaris et al., 2024) .

$$\epsilon_{CO_2} = \frac{\dot{m}_{CO_2}}{\dot{W}_{net}} \quad (16)$$

The CO_2 emission rate is estimated from the auxiliary power consumption of the air compressor and pumps using the electricity emission factor (Akroot & Al Shammre, 2024).

$$\dot{m}_{CO_2} = \gamma\left(\dot{W}_{AC} + \dot{W}_{P1} + \dot{W}_{P2}\right) \quad (17)$$

The parameter γ denotes the CO_2 emission factor for electricity generation and links electrical consumption to environmental impact; its value is 0.968 kg/kWh.

3. RESULTS AND DISCUSSIONS

The overall performance results presented in Table 2 demonstrate the capability of the proposed solar-driven CCHP system to produce electricity, cooling, and heating simultaneously. The BC provides the major share of power generation, with a work output of 5065 kW, while the ORC subsystem contributes an additional 1333 kW by recovering the remaining thermal energy from the Brayton cycle exhaust. As a result, the total net power output reaches 6397 kW, confirming the effectiveness of integrating the ORC as a bottoming cycle to enhance the power-generation capacity of the system. In addition to electricity production, the system delivers a cooling load of 2153 kW and a heating load of 747.5 kW, indicating its suitability for multigeneration applications, especially in regions with high cooling demand, such as Libya. The absorption refrigeration subsystem achieves a COP of 0.811, which reflects acceptable cooling performance for a single-effect LiBr–H_2O absorption cycle. The overall energy utilization factor is 63.44%, showing that a significant portion of the supplied solar energy is converted into useful outputs in the form of power, cooling, and heating. From the exergy perspective, the proposed system achieves an overall exergy efficiency of 47.54% and an electrical exergy efficiency of 46.8%. Also, the total exergy destruction rate of 6.946 MW shows that noticeable irreversibilities still occur within the integrated plant. The exergoeconomic results show that the total product cost is 22.48 $/MWh, while the cost of net electricity generation is 22.84 $/MWh. These relatively close values indicate that the system's economic performance is stable when considering both total useful products and electricity generation. Environmentally, the normalized CO_2 emission is 1.362 kg CO_2/MWh, which reflects the low emission potential of the solar-driven configuration, since the main energy input is supplied by solar radiation and emissions are mainly associated with auxiliary power consumption.

Table 1. Overall energy, exergy, exergoeconomic, and envitonmental performance of the proposed solar-driven CCHP system.

Aspect	**Symbol**	**Value**
BC work output (kW)	$\dot{W}_{BC}$	5065
ORC work output (kW)	$\dot{W}_{ORC}$	1333
Net power output (kW)	$\dot{W}_{net}$	6397
Heating load (kW)	$\dot{Q}_{heating}$	747.5
Cooling Load (kW)	$\dot{Q}_{cooling}$	2153
Overall energy utilization factor (%)	EUF	63.44
Overall exergy efficiency (%)	η_{ex}	47.54
Electrical energy utilization factor (%)	EUF_{elec}	43.65
Electrical exergy efficiency (%)	$\eta_{ex,ele}$	46.8
Coefficient Performance of ARS (-)	COP	0.811
Exergy destruction rate (MW)	$\dot{E}_d$	6.946
Economic performance of the system ($/MWh)	c_{Prod}	22.48
Economic performance of the net electricity generation ($/MWh)	c_{ele}	22.84
Normalized CO2 emission (Kg CO2/MWh)	ϵ	1.362

Table 3 presents the component-level exergy and exergoeconomic performance of the proposed solar-driven CCHP system. The results show that the solar receiver (SR) has the highest exergy destruction rate, reaching 3.838 MW, which represents the largest source of irreversibility in the system. The air compressor (AC) and gas turbine (GT) also show notable exergy destruction values of 0.803 MW and 0.879 MW, respectively. These losses are mainly associated with compression and expansion irreversibilities in the BC. However, their exergy efficiencies remain relatively high, with 91.05% for the compressor and 94.11% for the gas turbine, indicating that these components perform effectively from a thermodynamic perspective. Similarly, the ORC turbine (ORT) achieves a high exergy efficiency of 92.65%. Among the heat-transfer components, the recuperator records a high exergy efficiency of 97.6%, suggesting effective internal heat recovery within the Brayton cycle. In contrast, some low-temperature components, such as Condenser 1, the heater, the absorber, and the evaporator, show relatively low exergy efficiencies. For example, Condenser 1 has an exergy efficiency of only 11.13%, while the heater and absorber have efficiencies of 27.33% and 28.39%, respectively. Overall, the total exergy destruction rate of the system is 6.964 MW, while the overall exergy efficiency is 47.54%.

From the exergoeconomic perspective, the solar receiver has the highest cost associated with exergy destruction, with a value of 63.337 \$/h, making it the most critical component economically as well as thermodynamically. The ORC turbine and air compressor also contribute noticeably to the total exergoeconomic cost, with total cost rates of 14.7 \$/h and 14.72 \$/h, respectively. Overall, the total exergoeconomic cost rate reaches 146.1 \$/h, showing that component-level irreversibilities have a considerable influence on the economic performance of the plant. Therefore, the results of Table 3 highlight the solar receiver as the main component requiring improvement, followed by the compressor, gas turbine, and key heat-transfer units.

The exergoeconomic factor (f) indicates the relative contribution of investment cost compared with the cost of exergy destruction. As shown in Table 3, high f values are observed for the solar receiver and Pump 2 (100%), the recuperator (90.66%), and the ORC turbine (84.52%), suggesting that their costs are mainly dominated by capital investment. In contrast, very low f values are found for Condenser 1 (0.829%), the heater (2.195%), Condenser 2 (7.42%), and the generator (11.9%), indicating that exergy destruction has a stronger economic impact in these components. Overall, the total f value of 70.26% shows that investment-related costs dominate the overall system cost structure.

Table 2. Exergy and exergoeconomic results of the main components of the proposed solar-driven CCHP system

Parts	$\dot{\mathbf{E}}_{\mathbf{d}}$ (MW)	Ψ (%)	$\dot{\mathbf{C}}_{\mathbf{D,k}}$ (\$/h)	$\dot{\mathbf{Z}}_{\mathbf{k}}$ (\$/h)	$\dot{\mathbf{C}}_{\mathbf{k}}$ (\$/h)	$\boldsymbol{f}$ (%)
AC	0.803	91.05	5.819	8.897	14.72	60.46
Rec	0.03836	97.6	0.4001	3.886	4.286	90.66
SR	3.838	72.42	0	63.337	63.32	100
GT	0.879	94.11	5.523	7.997	13.52	59.15
HRVG	0.364	82.46	5.24	2.334	7.575	30.82
Heater	0.1187	27.33	3.638	0.08165	3.72	2.195
ORT	0.1082	92.65	2.275	12.43	14.7	84.52
Reg	0.09377	55.57	1.972	0.5858	2.558	22.9
$Cond_1$	0.3028	11.13	9.339	0.0781	9.418	0.8293
$Pump_1$	0.008868	71.91	0.2821	0.8666	0.9686	70.88
Gen	0.2525	70.96	3.636	0.4909	4.127	11.9
$Cond_2$	0.1215	27.37	2.555	0.2047	2.76	7.42
Ev_1	0.007536	93.08	0.2324	0	0.2324	0
Abs	0.05833	28.39	2.166	0.6304	2.796	22.54

$Pump_2$	0	100	0	0.00016	0.00016	100
SHEX	0.00332	89.62	0.7492	0.09881	0.1737	56.88
Ev_2	0.00016	99.97	0.0037	0	0.0037	0
Evap	0.1291	29.81	0.296	0.9223	1.218	75.71
Total	6.964	47.54	43.45	102.6	146.1	70.26

Figure 2 shows the effect of the Brayton cycle pressure ratio on the power output of the proposed solar-driven CCHP system. The findings show that increasing the Brayton cycle pressure ratio has a positive effect on the total power output of the proposed solar-driven CCHP system, although its effect on the ORC subsystem is very limited. As the Brayton cycle pressure ratio (PR) increases from 6 to 15, the Brayton cycle power output increases continuously from 4325 kW to 5521 kW. This increase shows that raising the pressure ratio improves the power-generation performance of the Brayton cycle because the gas turbine produces more useful work at higher pressure ratios. The ORC power output remains almost constant but shows a slight decreasing trend, changing from 1340 kW at PR = 6 to 1328 kW at PR = 15. The small decrease in ORC power output may be related to the reduction in the available exhaust heat from the Brayton cycle as more energy is converted into Brayton cycle power. The net power output of the whole CCHP system increases significantly from 5665 kW to 6849 kW as the pressure ratio increases from 6 to 15. At the design condition of PR = 10, the Brayton cycle produces 5065 kW, the ORC produces 1333 kW, and the total net power output reaches 6397 kW. The increase in net power output is mainly caused by the great improvement in Brayton cycle power, while the ORC contribution remains relatively stable.

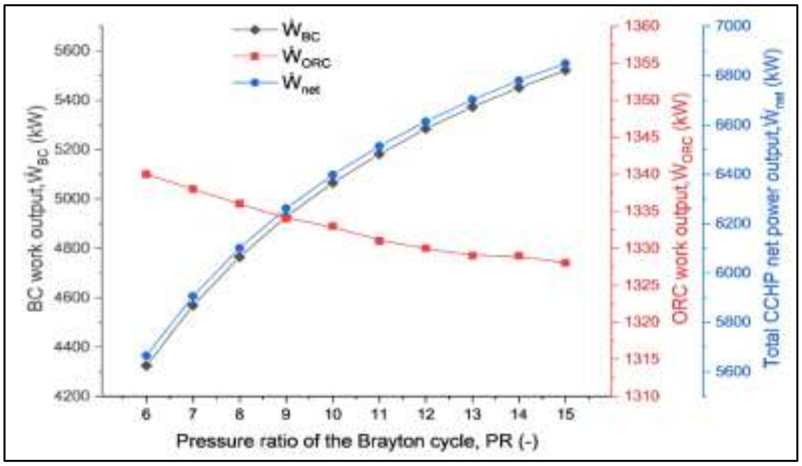

Figure 2. Effect of BC pressure ratio on the power outputs of the solar-driven CCHP system.

Figure 3 illustrates the effect of the Brayton cycle pressure ratio on the thermodynamic performance of the proposed solar-driven CCHP system. The results show a trade-off: increasing the pressure ratio improves power production and reduces exergy destruction, but it significantly reduces the heating capacity of the system. Increasing the Brayton cycle pressure ratio (PR) from 6 to 15 causes a clear decrease in the heating capacity of the system. The heating load decreases from 1451 kW at PR = 6 to 313.6 kW at PR = 15. This sharp reduction indicates that, at higher pressure ratios, more thermal energy is converted into power in the Brayton cycle, leaving less recoverable heat available for the heating unit. The cooling capacity shows only a slight decrease as the pressure ratio increases. The cooling load decreases from 2163 kW at PR = 6 to 2148 kW at PR = 15, which means that the absorption cooling subsystem is only weakly affected by the change in pressure ratio. At the base-case condition of PR = 10, the system provides 747.5 kW of heating and 2153 kW of cooling. The exergy destruction rate decreases from 7.635 MW at PR = 6 to 6.522 MW at PR = 15. This reduction in exergy destruction suggests that increasing the Brayton cycle pressure ratio improves the thermodynamic quality of energy conversion and reduces system irreversibilities.

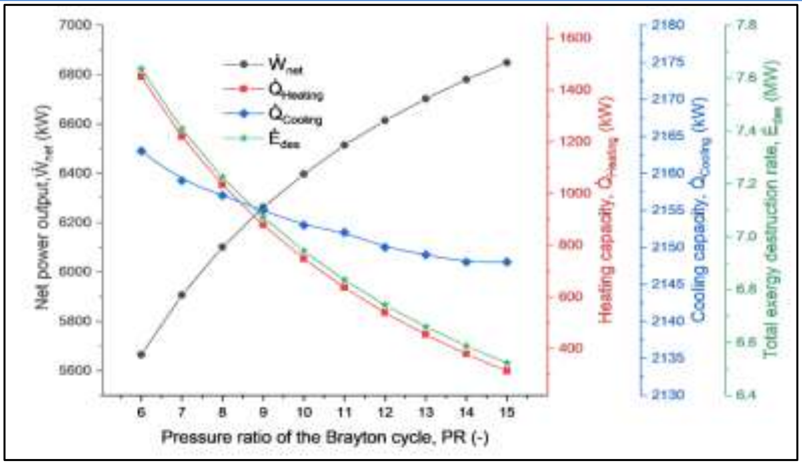

Figure 3. Effect of BC pressure ratio on the thermodynamic performance of the solar-driven CCHP system.

Figure 4 illustrates the influence of the Brayton cycle pressure ratio on the energy and exergy efficiency indicators of the proposed solar-driven CCHP system. The findings reveal that increasing the Brayton cycle pressure ratio has a strong positive effect on exergy-based and electricity-based performance indicators, while its effect on the overall energy utilization factor is limited. As the Brayton cycle pressure ratio (PR) increases from 6 to 15, the overall energy utilization factor increases only slightly from 63.31% to 63.52%. This small increase shows that the total useful energy output remains relatively stable, because the increase in power output is partly balanced by the decrease in heating capacity. The overall exergy efficiency improves clearly from 42.49% at PR = 6 to 50.64% at PR = 15. This improvement indicates that higher pressure ratios enhance the quality of energy conversion and reduce the relative impact of irreversibilities in the system. The electrical energy utilization factor increases from 38.65% to 46.73% as the pressure ratio rises from 6 to 15. The electrical exergy efficiency also increases from 41.44% to 50.10%, confirming that the system becomes more effective in converting available energy into electrical power. At the base-case condition of PR = 10, the system achieves an overall energy utilization factor of 63.44%, an overall exergy efficiency of 47.54%, an electrical energy utilization factor of 43.65%, and an electrical exergy efficiency of 46.8%. The highest efficiency values are obtained at PR = 15, where the overall exergy efficiency reaches 50.64%, and the electrical exergy efficiency reaches 50.10%.

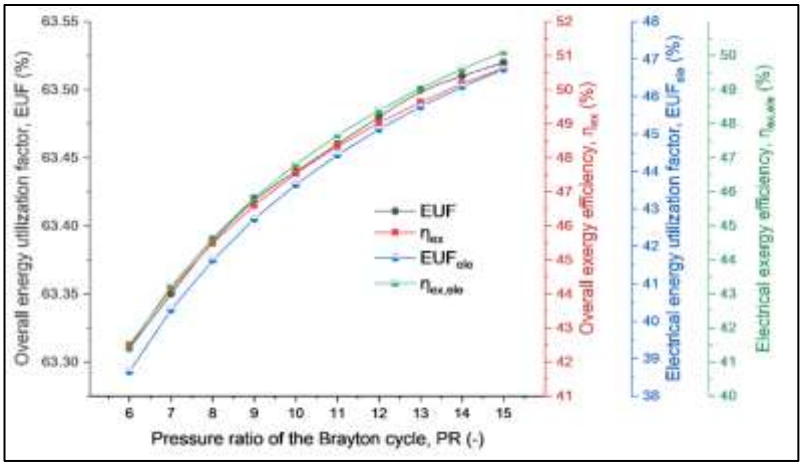

Figure 4. Effect of BC pressure ratio on the energy and exergy efficiency indicators of the solar-driven CCHP system.

Figure 5 presents the effect of the Brayton-cycle pressure ratio on the exergoeconomic and environmental performance indicators of the proposed solar-driven CCHP system. The results show that increasing the pressure ratio improves the exergoeconomic performance of the system by reducing product and electricity costs, but it also increases the normalized CO_2 emission. As the Brayton-cycle pressure ratio (PR) increases from 6 to 15, the total product cost generally decreases from 23.15 $/MWh to about 22.02 $/MWh. The electricity cost also decreases from 23.73 $/MWh at PR = 6 to 22.26 $/MWh at PR = 15. This reduction in cost is mainly related to the increase in net power output at higher pressure ratios, which improves the economic performance of the system. A slight increase in both cost indicators appears around PR = 10–11, where the total product cost rises from 22.48 to 22.50 $/MWh, and the electricity cost increases from 22.84 to 22.86 $/MWh. The lowest total product cost is observed around PR = 14, with a value of 22.01 $/MWh. The lowest electricity cost is obtained at PR = 15, with a value of 22.26 $/MWh. In contrast to the cost indicators, the normalized CO_2 emission increases continuously as the pressure ratio rises. The emission value increases from 1.108 kg CO_2/MWh at PR = 6 to 1.592 kg CO_2/MWh at PR = 15. At the base-case condition of PR = 10, the system records a total product cost of 22.48 $/MWh, an electricity cost of 22.84 $/MWh, and a normalized CO_2 emission of 1.362 kg CO_2/MWh.

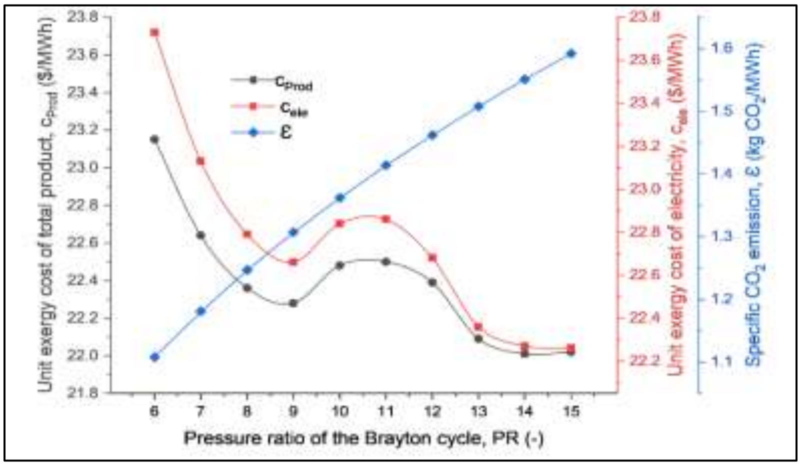

Figure 5. Effect of Brayton-cycle pressure ratio on the exergoeconomic and environmental performance indicators of the solar-driven CCHP system.

Figure 6 illustrates the effect of the ORC turbine inlet temperature on the power outputs of the proposed solar-driven CCHP system. The findings present that as the ORC turbine inlet temperature increases from 290 to 335, the Brayton cycle power output remains constant at 5065 kW. This indicates that changing the ORC turbine inlet temperature does not affect the Brayton cycle, because the Brayton cycle operates as the topping cycle. The ORC power output increases gradually from 1310 kW at T = 290 to 1392 kW at T = 335. This increase occurs because higher ORC turbine inlet temperature improves the expansion process and allows the ORC turbine to generate more power. The net power output also increases from 6375 kW to 6457 kW as the ORC turbine inlet temperature increases. The improvement in net power output is mainly due to the increase in ORC power output, since the Brayton cycle power remains unchanged.

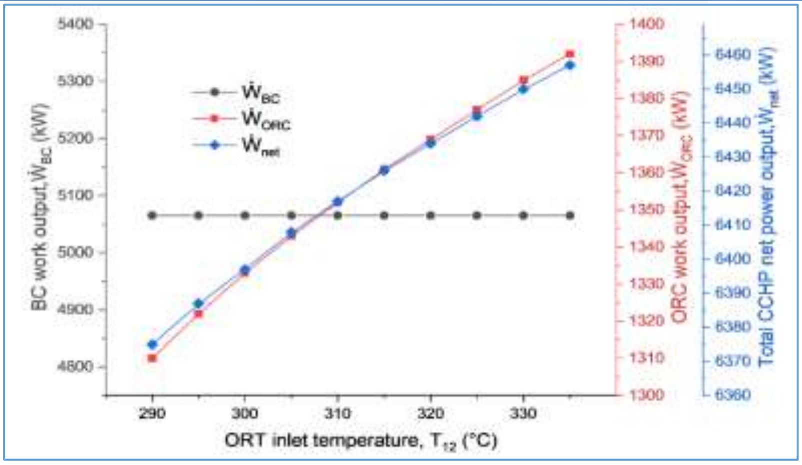

Figure 6. Effect of ORC turbine inlet temperature on the power outputs of the solar-driven CCHP system.

Figure 7 illustrates the effect of the ORC turbine inlet temperature on the thermodynamic performance of the proposed solar-driven CCHP system. The findings show that the ORC turbine inlet temperature mainly affects the thermodynamic quality of the system through a slight reduction in irreversibilities, while the useful heating and cooling outputs remain stable. As the ORC turbine inlet temperature increases from 290 to 335, the heating capacity remains constant at 747.5 kW. The cooling capacity also remains unchanged at 2153 kW over the entire temperature range. This indicates that changing the ORC turbine inlet temperature has no noticeable effect on the heating and cooling outputs of the system. Although the heating capacity and cooling capacity remain constant as the ORC turbine inlet temperature increases, the net power output increases from 6375 kW to 6457 kW. This means that the improvement in system performance is mainly reflected in electricity generation rather than in heating or cooling production. In contrast, the exergy destruction rate decreases gradually from 6.970 MW at T = 290 to 6.882 MW at T = 335. This reduction in exergy destruction shows that increasing the ORC turbine inlet temperature slightly improves the thermodynamic performance of the system. At the base-case condition of T = 300, the exergy destruction rate is 6.946 MW, while the heating and cooling loads remain 747.5 kW and 2153 kW, respectively.

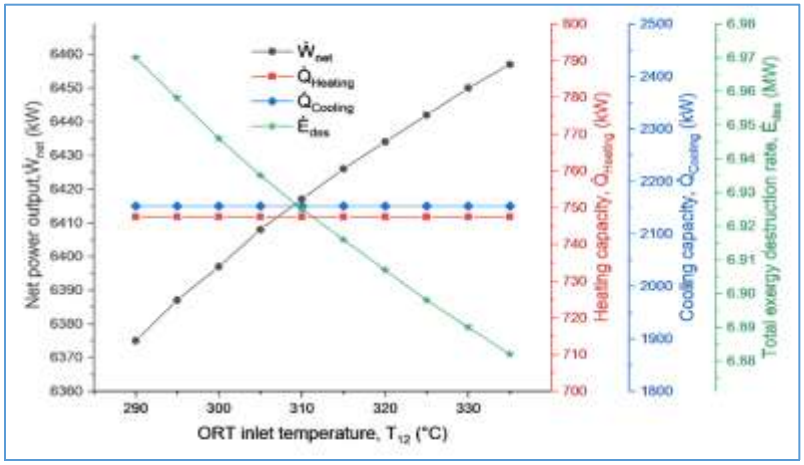

Figure 7: Effect of inlet ORT temperatures on the thermodynamic performance of the solar-driven CCHP system

Figure 8 shows the effect of the ORC turbine inlet temperature on the energy and exergy efficiency indicators of the proposed solar-driven CCHP system. Increasing the ORC turbine inlet temperature has a positive but limited effect on the energy and exergy efficiency performance of the proposed solar-driven CCHP system. As the

ORC turbine inlet temperature increases from 290 to 335, all efficiency indicators increase gradually. The overall energy utilization factor (ETF) increases slightly from 63.29% to 63.85%. The overall exergy efficiency rises from 47.37% to 47.97%, showing a modest improvement in the quality of energy conversion. The electrical energy utilization factor (ETF_ele) increases from 43.50% to 44.06%. The electrical exergy efficiency also improves from 46.64% to 47.24%. At the base-case condition of T = 300, the system records 63.44% ETF, 47.54% overall exergy efficiency, 43.65% electrical energy utilization factor, and 46.80% electrical exergy efficiency. The improvement is mainly related to the increase in ORC power output, which enhances the net power output while the Brayton cycle, heating, and cooling outputs remain nearly unchanged.

Figure 9 illustrates how the ORC turbine inlet temperature affects the exergoeconomic and environmental performance indicators of the proposed solar-driven CCHP system. Increasing the ORC turbine inlet temperature improves both the economic and environmental performance of the system. As the ORC turbine inlet temperature rises from 290 to 335, the total product cost gradually declines from 22.56 $/MWh to 22.36 $/MWh. The electricity cost also decreases from 22.92 $/MWh at T = 290 to 22.71 $/MWh at T = 335. This reduction indicates that higher ORC turbine inlet temperatures improve the system's exergoeconomic performance. The improvement is primarily due to increased ORC and net power output, which lowers the unit cost of the useful products and electricity generation. The normalized CO_2 emission decreases slightly from 1.367 kg CO_2/MWh to 1.349 kg CO_2/MWh as the inlet temperature increases. This trend shows a slight improvement in the system's environmental performance at higher ORC turbine inlet temperatures. At the base-case condition of T = 300, the system records a total product cost of 22.48 $/MWh, an electricity cost of 22.84 $/MWh, and a normalized CO_2 emission of 1.362 kg CO_2/MWh.

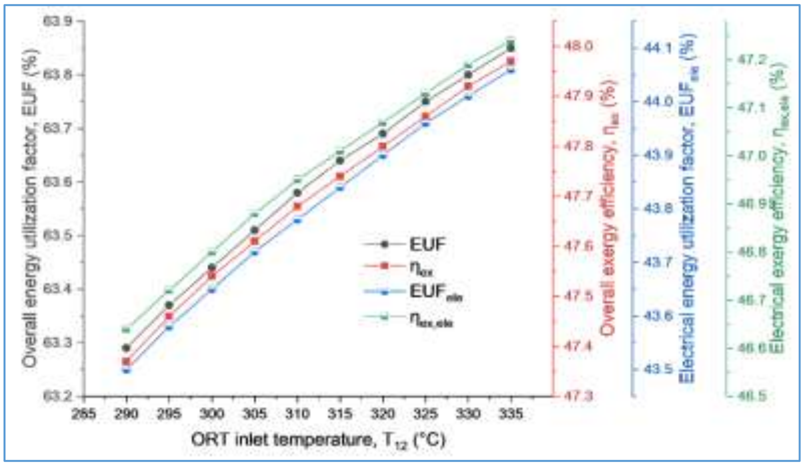

Figure 8. Effect of ORC turbine inlet temperature on the energy and exergy efficiency indicators of the solar-driven CCHP system.

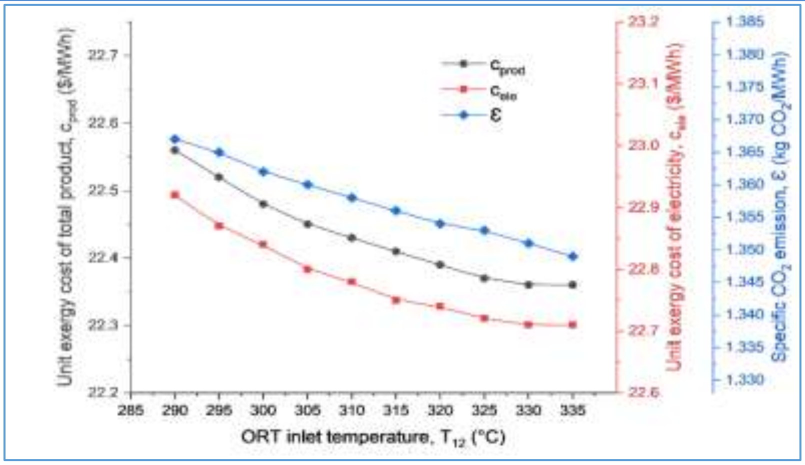

Figure 9. Effect of inlet ORT temperatures on the exergoeconomic and environmental performance indicators of the solar-driven CCHP system.

4. CONCLUSION

This study evaluated a solar-driven combined cooling, heating, and power (CCHP) system for operation under the climatic conditions of Tripoli, Libya. The proposed configuration combines a solar-assisted Brayton cycle, an organic Rankine cycle, a LiBr–H_2O absorption cooling subsystem, and a heating unit. The system was assessed from energy, exergy, exergoeconomic, and environmental perspectives using EES simulation.

The base-case results showed that the system produces 6397 kW of net power, 2153 kW of cooling, and 747.5 kW of heating. The overall energy utilization factor and overall exergy efficiency were 63.44% and 47.54%, respectively, while the absorption cooling subsystem achieved a COP of 0.811. The economic results showed a total product cost of 22.48 $/MWh and an electricity cost of 22.84 $/MWh, with a normalized CO_2 emission of 1.362 kg CO_2/MWh.

The parametric results indicated that increasing the Brayton cycle pressure ratio improves power output and exergy efficiency but reduces heating capacity and increases CO_2 emissions. Increasing the ORC turbine inlet temperature slightly improves power output, efficiencies, cost performance, and environmental behavior. Overall, the proposed solar-driven CCHP system shows good potential for sustainable multigeneration applications in Libya and similar solar-rich regions.

SYMBOLS AND ABBREVIATIONS INDEX

Symbols	
$\dot{C}$	cost rate ($/hr or $/s)
$\dot{Z}$	capital investments
$\dot{E}$	exergy (kW)
$\dot{Q}$	heat transfer (kW)
$\dot{W}$	work done (kW)
c	unit exergy cost ($/GJ, $/kWh, $/MWh)
COP	coefficient of performance
EUF	Electrical energy utilization factor
f	Exergoeconomic factor (%)
T	temperature (°C)
Greek symbols	
ŋ	efficiency (%)
γ	CO_2 emission factor
ψ	exergy efficiency (%)
ϵ	Normalized CO2 emission (Kg CO2/MWh)
Subscripts	
D	destruction
ele	electricity
ex	exergy
Prod	product
Abbreviations	
Abs	absorber
AC	compressor
ARC	absorption refrigeration cycle
BC	Brayton cycle
CCHP	combined cooling, heating, power
Cond	condenser
Ev	expansion valve
Evap	evaporator
Gen	generator
GT	gas turbine
HRVG	heat recovery vapor generation
ORC	Organic Rankine cycle
ORT	Organic Rankine turbine
P	pump
Rec	recuperator
Reg	regenerative
SHES	sensible heat exchanger
SR	solar reservoir

KAYNAKLAR

Aieneh, K., Mehranfar, S., Yazdi Sotoude, M., Sadeghi, S., & Mahmoudzadeh Andwari, A. (2024). Solar-Powered Combined Cooling, Heating, and Power Energy System with Phase-Change Material and Water Electrolysis: Thermo-Economic Assessment and Optimization. *Energies*, *17*(13), 3309.

Akroot, A. (2025). Thermodynamic and Environmental Performance Analysis of the Marib Integrated Power and Cooling Cycle (MIPCC). *Black Sea Journal of Engineering and Science*, *8*(3), 814–823. https://doi.org/10.34248/bsengineering.1627614

Akroot, A., & Al Shammre, A. S. (2024). Techno-Economic and Environmental Impact Analysis of a 50 MW Solar-Powered Rankine Cycle System. *Processes*, *12*(6), 1059. https://doi.org/10.3390/pr12061059

Akroot, A., Almohammedi, A. A., & Talal, W. (2026). Design and Analysis of a Solar-Assisted Combined Cooling, Heating, and Power System for Smart Cities: Case Study From Doha. In *Challenges for Smart City Infrastructure, Technologies, and Their Future* (pp. 123–146). IGI Global Scientific Publishing. https://doi.org/10.4018/979-8-3373-0154-9.ch006

Akroot, A., & Refaei, M. (2025). Thermodynamic and Exergoeconomic Assessment of a Solar-Assisted Combined Cooling, Heating, and Power System in Antalya, Turkey. *Gazi Üniversitesi Fen Bilimleri Dergisi Part C: Tasarım ve Teknoloji*, 1.

Alfaris, A., Akroot, A., Alqaed, S., & Almehmadi, F. A. (2025). Performance analysis of integrated solar and natural gas combined cycle power plants in high solar potential regions. *Scientific Reports*, *15*(1), 9181.

Alfaris, A., Akroot, A., & Deniz, E. (2024). The Exergo-Economic and Environmental Evaluation of a Hybrid Solar–Natural Gas Power System in Kirkuk. *Applied Sciences*, *14*(22), 10113. https://doi.org/10.3390/app142210113

Cho, H., Smith, A. D., & Mago, P. (2014). Combined cooling, heating and power: A review of performance improvement and optimization. *Applied Energy*, *136*, 168–185. https://doi.org/10.1016/J.APENERGY.2014.08.107

Deniz, E., & Çınar, S. (2016). Energy, exergy, economic and environmental (4E) analysis of a solar desalination system with humidification-dehumidification. *Energy Conversion and Management*, *126*, 12–19. https://doi.org/10.1016/J.ENCONMAN.2016.07.064

Eshtaiwi, S., Aburwais, M., Elsanusi, O., Elayeb, M., & Shetwan, M. (2022). The Impact of Residential Optimally Designed Rooftop PV System on Libya Power Shortage Case. *Journal of Energy: Energija*, *71*(3.), 3–9.

García-Domínguez, J., Blanco-Marigorta, A. M., & Daniel Marcos, J. (2023). Analysis of a solar driven ORC-absorption based CCHP system from a novel exergy approach. *Energy Conversion and Management: X*, *19*, 100402. https://doi.org/10.1016/J.ECMX.2023.100402

Gnedi, M. D., & Robaa, S. M. (2024). Extreme climate indices over Libya: current and future outlooks. In *Hydroclimatic Extremes in the Middle East and North Africa* (pp. 343–366). Elsevier.

Jiménez-García, J. C., Moreno-Cruz, I., & Rivera, W. (2024). Thermodynamic Modeling of a Solar-Driven Organic Rankine Cycle-Absorption Cooling System for Simultaneous Power and Cooling Production. *Processes*, *12*(3). https://doi.org/10.3390/pr12030427

Kareem, A. F., Akroot, A., Abdul Wahhab, H. A., Talal, W., Ghazal, R. M., & Alfaris, A. (2023). Exergo–Economic and Parametric Analysis of Waste Heat Recovery from Taji Gas Turbines Power Plant Using Rankine Cycle and Organic Rankine Cycle. *Sustainability (Switzerland)*, *15*(12). https://doi.org/10.3390/su15129376

Khalil, A., Rajab, Z., Amhammed, M., & Asheibi, A. (2017). The benefits of the transition from fossil fuel to solar energy in Libya: A street lighting system case study. *Applied Solar Energy*, *53*, 138–151.

Liu, M., Shi, Y., & Fang, F. (2014). Combined cooling, heating and power systems: A survey. *Renewable and Sustainable Energy Reviews*, *35*, 1–22. https://doi.org/10.1016/j.rser.2014.03.054

Pokson, C., & Chaiyat, N. (2022). Thermal performance of a combined cooling, heating, and power (CCHP) generation system from infectious medical waste. *Case Studies in Chemical and Environmental Engineering*, *6*(June). https://doi.org/10.1016/j.cscee.2022.100221

P.P. da Silva, R., Strobel, M., Erguvan, M., & Amini, S. (2025). 3E analysis of a solar hybrid CCHP system at a university campus. *Solar Energy*, *291*, 113413. https://doi.org/10.1016/J.SOLENER.2025.113413

Shi, Y., Liu, M., & Fang, F. (2017). *Combined cooling, heating, and power systems: modeling, optimization, and operation*.

Talal, W., & Akroot, A. (2023). Exergoeconomic Analysis of an Integrated Solar Combined Cycle in the Al-Qayara Power Plant in Iraq. *Processes*, *11*(3). https://doi.org/10.3390/pr11030656

Talal, W., & Akroot, A. (2024). An Exergoeconomic Evaluation of an Innovative Polygeneration System Using a Solar-Driven Rankine Cycle Integrated with the Al-Qayyara Gas Turbine Power Plant and the Absorption Refrigeration Cycle. *Machines*, *12*(2), 133. https://doi.org/10.3390/machines12020133

Tawil, I., Abeid, M., Abraheem, E., Alghoul, S., & Dekam, E. (2018). Review on solar space heating-cooling in Libyan residential buildings. *Solar Energy and Sustainable Development Journal*, *7*(SI), 78–112.

Wang, J., Dai, Y., Gao, L., & Ma, S. (2009). A new combined cooling, heating and power system driven by solar energy. *Renewable Energy*, *34*(12), 2780–2788. https://doi.org/10.1016/J.RENENE.2009.06.010

Wang, J., Han, Z., & Guan, Z. (2020). Hybrid solar-assisted combined cooling, heating, and power systems: A review. *Renewable and Sustainable Energy Reviews*, *133*, 110256. https://doi.org/10.1016/J.RSER.2020.110256

Wu, D. W., & Wang, R. Z. (2006). Combined cooling, heating and power: A review. *Progress in Energy and Combustion Science*, *32*(5–6), 459–495. https://doi.org/10.1016/j.pecs.2006.02.001

Zarei, A., Akhavan, S., Rabiee, M. B., & Elahi, S. (2021). Energy, exergy and economic analysis of a novel solar driven CCHP system powered by organic Rankine cycle and photovoltaic thermal collector. *Applied Thermal Engineering*, *194*, 117091. https://doi.org/10.1016/J.APPLTHERMALENG.2021.117091

Zhang, N., Wang, Z., & Han, W. (2017). Analysis of A Solar Assisted Combined Cooling, Heating and Power (SCCHP) System. *Energy Procedia*, *142*, 55–62. https://doi.org/10.1016/j.egypro.2017.12.010

Zhao, L., Zhang, Y., Deng, S., Ni, J., Xu, W., Ma, M., Lin, S., & Yu, Z. (2018). Solar driven ORC-based CCHP: Comparative performance analysis between sequential and parallel system configurations. *Applied Thermal Engineering*, *131*, 696–706. https://doi.org/10.1016/J.APPLTHERMALENG.2017.12.028

Zhao, X., Yang, S., Liu, Z., Wang, D., Du, Z., & Ren, J. (2024). Optimization and exergoeconomic analysis of a solar-powered ORC-VCR-CCHP system based on a ternary refrigerant selection model. *Energy*, *290*, 129976. https://doi.org/10.1016/J.ENERGY.2023.129976